Int. J. Nanosci. Nanotechnol., Vol. 17, No. 2, June 2021, pp. 109-121

Role of Green Synthesized CuO Nanoparticles of Trigonella Foenum-Graecum L. Leaves and their Impact on Structural, Optical and Antimicrobial Activity

S. P. Lakshmanan[1], S. T. Jostar[1,*], G. J. Arputhavalli[2], S. Jebasingh[3] and C. M. R. Josephine[4]

[1]PG & Research Department of Physics, Sadakathullah Appa College, Tirunelveli, India
[2]Department of Physics, Coimbatore Institute of Technology, Coimbatore, India
[3]Department of Mathematics, Karunya Institute of Technology and Sciences, Coimbatore, India
[4]Department of Life Sciences, Kristu Jayanti College (Autonomous), Bengaluru, India

(*) Corresponding authors: saintajostar85@gmail.com
(Received: 22 December 2020 and Accepted: 21 March 2021)

Abstract

The present research work focused on the synthesis, characterization and testing of antimicrobial activity of CuO nanoparticles prepared by green synthesis method using Trigonella foenum-graecum L. leaf extract. The XRD pattern indicated the presence of cubic structure of nanocrystalline CuO with crystallite size of 47 nm. The optical band gap was calculated using Tauc's plot and found to be 3.6 eV. SEM images revealed that the particles had cluster structures with a combination of different shapes. EDAX analysis confirmed the presence of copper and oxide by indicating predominant peak which was the highest percentage present in the spectrum. The synthesized nanoparticles showed significant antibacterial and antifungal activity against the human pathogens Staphylococcus aureus and Penicillium sp. So this nanoparticle can be considered as an alternate approach for reducing the adhesion of micro-organisms.

Keywords: *CuO, Green synthesis, Structural properties, Morphological, Antimicrobial activity.*

1. INRODUCTION

Nanotechnology is an important technology in advanced research field because of its several uses from material scientist and engineering. It includes many applications in the field of energy science, electronics, mechanics, cosmetics, bio-medical science, chemical industries, etc. In recent years, nanoparticles are used to replace the bulk material and it is an expanding field due to their different properties [1, 2, 3]. The oxidative nanoparticles are suitable for mechanical, optical, gas sensing and electromagnetic applications. Due to their extraordinary properties, Copper oxide (CuO) nanoparticles are considered as a multi-task metal oxide with good physical, chemical and biological properties. Moreover, its stability, non-toxicity and abundance are also other benefits of this material to be explored for several applications [4]. CuO nanoparticles have been widely used in various fields such as optoelectronics, catalysis, nanosensor, information storage [5], lithium-ion batteries [6], cosmetics, drugs, solar cells and microbiology applications. These nanoparticles are reported as safe and less toxic; hence it has been used to treat diseases caused by bacteria, fungi as well infections of the urinary tract [7]. Synthesis and application of nanomaterials

are important in the scientific and industrial zone due to their unique properties which were predominantly determined by size, composition and structure. These properties were strongly correlated to the preparation methods [8, 9]. Thus the synthesis of nanoparticle is a fundamental step which includes various chemical, physical and biological techniquees such as microbe based and plant based green synthesis [10, 11]. The chemical and physical techniques may absorb some of the toxic compounds on the nanoparticle surface that have changed the medicinal properties. So among these techniques, green synthesis of nanoparticles using plant leaf extract is favourable for the reason of easy, fast, non-toxic and economically reliable [1,12].

Synthesis of CuO nanoparticles from plant extract is a green synthesis, which creates a strong bond between plant and nano material synthesis [13]. In the literature several plant leaves such as *Abutilon indicum* [14], *Aloe vera* [15], *Malva sylvetris* [16], *Psidium guajava* [17], *Lantana camara* [18] and *Gloriosa superb* [19], *Solanum nigrum* [20], *Terminalia phanerophlebia* [21], were used for the preparation of CuO. So, CuO nanoparticle could be obtained through the process of plant leaf extraction. This phytomediated method using different plant extract is considered to be a novel, modest and inexpensive approach to prepare metal nanoparticles. For this purpose, *Trigonella foenum-graecum* L. plant leaf extract was used as a reducing or capping agent for green synthesis of CuO nanoparticles due to the existence of huge quantity of bioactive compounds. The leaf extract from this plant has been used in traditional medicines like balancing cholesterol, diabetes, digestion, etc. It also finds applications in food additives, drugs, perfumes and cosmetics.

In [22], the authors exhibited that the size and surface morphology of the nanoparticles were strongly influenced by the plant material in the green synthesis. Also the results presented in [23] shows that green synthesis of nanoparticles are larger in size compared to the size of the nanoparticles obtained by chemical methods.

In [24], the authors have studied copper oxide nanoparticles and its application to treatment of wounds and virus infections. In the treatment of wounds on human body, bacteria's such as *Staphylococcus aureus, Escherichia coli, Klebsiella pneumoniae,* and *Salmonella typhimurium* were known to aggravate the damaged tissues and cause delay in the healing of wounds. However these pathogenic bacteria's can be subjugated by the CuO nanoparticles. The CuO particles are also used efficiently in the clinical treatment of hepatitis A viruses and influenza as antiviral agent. In [25], the authors exhibited that CuO nanoparticles were compatible with living tissue. The study proved that on human cancer cell lines the composite had insignificant toxicity, for below 100 μg/mL of Cu content. Also, it was showed that the lower concentrations of CuO composite nano particles were balanced by its biocompatibility with human fibroblasts. Hence it can be used for therapeutic purposes such as treatment of variety of microbial infections.

With this background, the present work focused on a cost-effective, simple and eco-friendly synthesis of CuO nanoparticles using *Trigonella foenum-graecum* L. plant through green synthesis. The study highlighted on the economical and cost effective approach for the synthesis of CuO nanoparticles due to their vital nature and remarkable antimicrobial activity.

2. EXPERIMENTAL DETAILS

2.1. Preparation of Extract Solution

The schematic diagram for the green synthesis of CuO nanoparticles from plant extract is depicted in Figure 1. The fresh leaves of *Trigonella foenum-graecum* L. plant were collected from paddy field in Puliyankulam village of Thoothukudi,

Tamilnadu. The collected leaves were washed thoroughly using running tap water and double distilled water to remove the adhering soil and other dust particles. 50g of the leaf sample was taken and ground in a sterile Pestle and Mortar using distilled water as the solvent. The macerated leaf sample was then filtered using Whatman No.1 filter paper in order to get *Trigonella foenum-graecum* L. leaf extract solution. This solution was used for the reduction of copper ions.

2.2. Synthesis of CuO Nanoparticles

All the chemicals used in this experiment were of analytical grade without further purification. CuO nanoparticles were prepared at room temperature by chemical route using green synthesis technique. In a typical synthesis route, a precursor solution was prepared by dissolving 0.1M of copper sulfate in 200ml of distilled water which was then added with 25ml of the fresh leaf extract solution. The solution was continuously stirred for 4 h till a precipitate formed in the bottom of the beaker. The obtained precipitate was washed with deionized water and filtered using Whatman No.1 filter paper for removing the carbon residue. The washed precipitates were dried at 80°C for 24 h and the gained 2.5 gram nanoparticles were calcined at 500°C for 2 h in order to obtain the 2 grams of crystalline nature of CuO.

2.3. Characterization Techniques

The phase of as-synthesized CuO nanopowders were recorded by powder X-ray diffraction using analytical PANalytical X'Pert Pro of Cu Kα radiation with a scanning rate of 2° per minute ranging from 30° to 80°. Surface morphology and composition of the sample was analyzed by scanning electron microscopy (SEM) with EDAX performed on HITACHI S3400N. The formation of CuO and their functional groups were confirmed using Fourier Transform Infrared Spectroscopy (FTIR) which was carried out on a Perkin Elmer Spectrophotometer (Model: Spectrum 1000). The optical properties of the nanoparticles were recorded using Perkin Elmer Lambda 35 UV-Visible spectrophotometer.

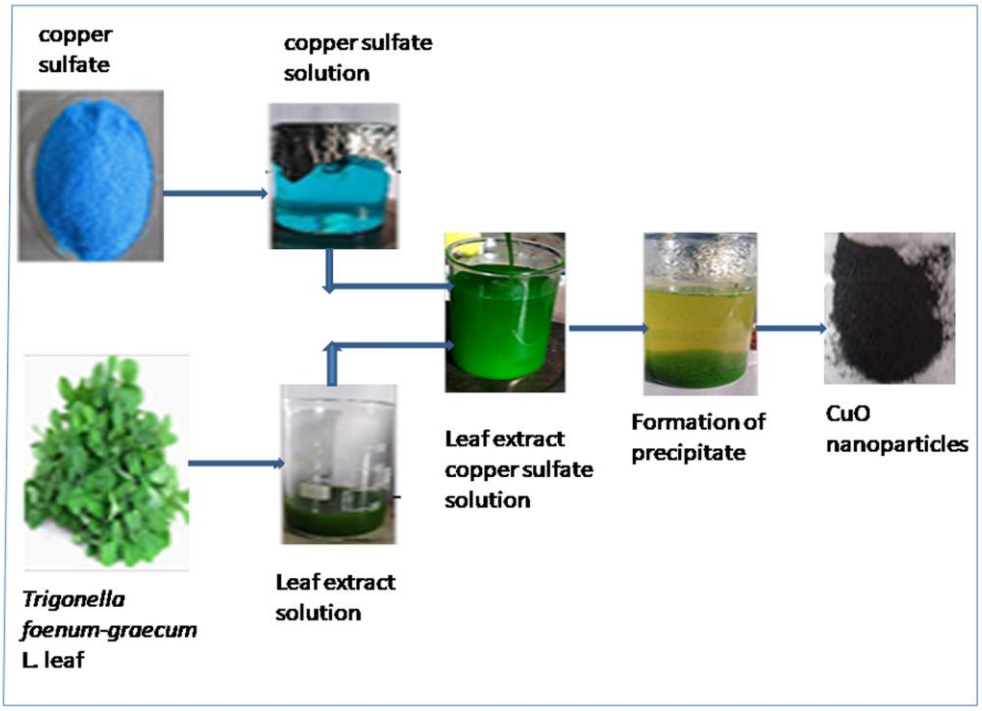

Figure 1. *Schematic diagram of green synthesized CuO nanoparticles from plant extract.*

Photoluminescence emission spectra of the prepared CuO nanoparticles were examined using photoluminescence spectrometer. The antimicrobial activity of the nanoparticle was determined by testing its efficacy against the bacterial pathogen *Staphylococcus aureus* [26] at various concentrations by the well diffusion method. Minimum inhibitory concentration was determined by microbroth dilution technique. Different concentrations of the CuO nanopowders at various concentrations were tested against the fungus *Penicillium* sp. to determine its antifungal potential. Each test was repeated three times, and the resulting bacterial growth on three plates was taken, their corresponding average values and standard deviation were reported in table 3.

3. RESULTS AND DISCUSSION

3.1. Structural Analysis

The XRD pattern showed the presence of a sharp band of Bragg's peak of CuO nanoparticles may be due to the stabilization of the nanoparticle by a mixture of reducing agent of the leaf extract (*Trigonella foenum-greacum* L.). This clearly illustrated that the CuO nanoparticles were synthesized by green synthesis method and it was nanocrystalline in nature.

XRD pattern confirmed the formation of CuO nanoparticles with five diffraction peaks at 2θ= 36.61°, 43.47°, 50.63°, 61.52° and 74.26° which are ascribed to (111), (200), (211), (220) and (311) planes respectively as shown in Figure 2. All the diffraction peaks corresponded to CuO nanoparticles that well matched with the JCPDS file (No: 780428) which showed that it belonged to the face centered cubic CuO phase. No other phase of impurity peak was reflected from the XRD pattern.

The observed and theoretical values of hkl reflections from XRD peak indexing and d-spacing are tabulated in Table 1.

Table 1. *XRD Peak Indexing of CuO nanoparticles.*

Peak Position			**Reflection (hkl)**	**d-spacing**		
(2θ deg)	**1000 * $\sin^2$ θ**	**1000 * $\sin^2$ θ/33**		**d-spacing nm**	**1000/d^2**	**(1000/d^2)/55.79**
36.61	98	3	(111)	2.45	166.05	3
43.47	137	4	(200)	2.08	230.74	4
50.63	183	6	(211)	1.80	307.64	6
61.52	261	8	(220)	1.51	440.17	8
74.26	364	11	(311)	1.28	613.06	11

Table 2. *Structural profile of CuO nanoparticles.*

(2θ deg)	**FWHM (β) radians**	**Lattice constant (a) Å**	**Scherrer Method**			**Specific surface area (m^2 g^{-1}) 10^{10}**	**Number of unit cell 10^5**	**Cell volume (V) (nm^3)**
			Crystallite size (D) nm	**Micro strain(ε) 10^{-3}**	**Dislocation density (δ) lines/m^2 10^{14}**			
36.61	0.0064	4.2505	21	1.60	21.44	4.40	0.69	76.79
43.47	0.0015	4.1635	95	0.36	1.11	1.00	5.89	72.17
50.63	0.0030	4.1632	47	0.72	4.43	2.00	4.45	72.16
61.52	0.0093	4.2632	14	2.33	45.35	6.39	0.22	77.48
74.26	0.0024	4.2358	58	0. 58	2.83	1.60	14.36	75.99

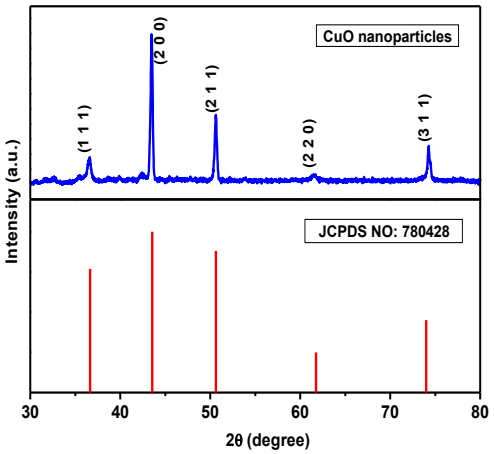

Figure 2. *XRD pattern of synthesized CuO nanoparticles.*

The experimental results discussed here were found to be in agreement with the reported diffraction patterns of CuO [27] nanoparticles by fruit and leaf extract. The grain size of copper oxide nanoparticles was calculated from the full width at half maximum (FWHM) of the major peaks using the following Scherer formula,

$$D = \frac{0.9\lambda}{\beta \cos(\theta)} \qquad (1)$$

where, λ is the wavelength of X-Ray (0.1541 nm), β is FWHM, θ is the Bragg diffraction angle and D is the crystallite size [28]. The crystallite size of the CuO nanoparticles obtained from full-width at half maximum of the diffraction peak was 47 nm. The strain *(ε)* induced in nanoparticles due to distortion and imperfection of crystal can be calculated and their values are given in Table 2.

$$\varepsilon = \frac{\beta \cos(\theta)}{4} \qquad (2)$$

The dislocation density (δ) values can be calculated using the following equation

The dislocation density describes the length of dislocation lines per unit volume of the crystal. It shows the presence of irregularity or crystallographic defect within a crystal structure. The higher value of dislocation density represents a higher hardness of the material [29].

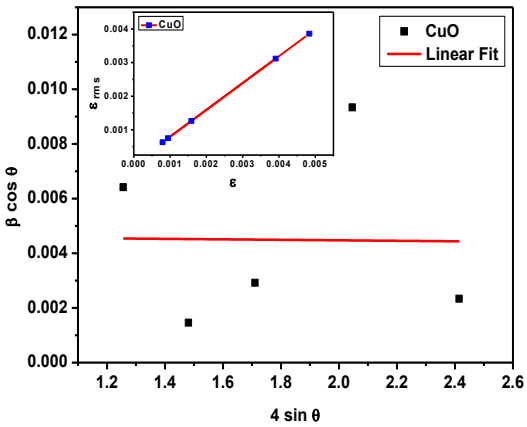

Figure 3. *W- H plot of synthesized CuO nanoparticles.* ***(insight)*** *shows the* ε_{rms} *verses ε of CuO nanoparticles.*

$$\delta = \frac{1}{D^2} \qquad (3)$$

The dislocation density of the CuO nanoparticle is indirectly proportional to particle size and number of unit cell. The calculated structural parameters such as crystallite size, micro strain and dislocation density of prepared CuO nanoparticles were tabulated in Table 2. It shows that the dislocation density and micro strain of the nanoparticle increases but the grain size decreases. The important factors such as shape, density and particle size were correlated to the quantity of specific surface area ($m^2 . g^{-1}$). The particle specific surface area can be calculated by

$$SSA = 6*10^3/D_p*\rho \qquad (4)$$

where D_p is the particle size and ρ is the density of the CuO nanoparticles. The number of unit cell can be calculated by

$$N = (4/3)*(D/2)^3*(1/V) \qquad (5)$$

where D is the crystallite size and V is the cell volume of the sample. It is observed that the dislocation density increases while both grain size and number of unit cell decreases. Lattice constant can be calculated by

$$d = \left[\frac{a}{\sqrt{h^2 + k^2 + l^2}} \right] \qquad (6)$$

where *a* is the lattice constant, *d* is the d-spacing value and *h, k* and *l* are Miller indices for the particular Bragg reflection of the nanoparticle. The cell volume (*V*) can also be calculated using the equation (7).

$$V=a^3 \quad (7)$$

The calculated lattice constant *a* (4.215 A°) and cell volume *V* (74.92) values are perfectly matched with the standard JCPDS data (*a*= 4.245 A° and *V*= 76.49). The calculated values of structural parameters such as specific surface area, number of unit cell, lattice constant and cell volume of CuO nanoparticles were tabulated in Table 2.

Scherrer formula determines only the effect of grain size on the XRD peak broadening and it doesn't determine about the lattice microstructures. The Williamson-Hall (W-H) method is commonly used for the determination of grain size and the nature of strain induced to line broadening in the nanoparticles [30]. A plot was drawn between 4sinθ along the x-axis and βcosθ along the y-axis for prepared CuO nanoparticles as shown in Figure 3. Using linear fit to the data, lattice strain and grain size was estimated from the slope and y-intercept of the fitted line respectively. The W- H plot of prepared CuO nanoparticles showed that the lattice strain was assumed to be uniform in all crystallographic directions representing the isotropic nature of the crystal. The insight plots of Figure 3., shows that ε_{rms} linearly varies with ε also confirms that the strain is assumed to be same with all crystallographic lattice planes [31].

Thus, the prepared CuO nanoparticle characteristics were independent of the direction along which they could be measured. The lattice strain occurs in the nanoparticle shows lattice expansion or contraction in the nanocrystals due to size confinement (i.e., the atomic arrangement possesses a little modification due to size confinement compared to their bulk counterpart). Conversely, many defects are also formed in the lattice structure due to the size confinement, which results in the lattice strain [32]. The grain size observed from the W-H plot is 40 nm which is in good agreement with the value obtained from the Scherrer formula. The slope of the W-H plot shows a positive value indicates the presence of lattice expansion, which may produce an intrinsic strain in the nanocrystals. The calculated intrinsic strain from the slope was found to be 4. 65x 10^{-3}.

3.2. Optical Analysis

The absorption spectrum of the prepared CuO nanoparticles was investigated at room temperature to obtain information about the energy band and the type of electronic transitions. The absorption coefficient α was calculated from the measured transmittance spectra of the prepared nanoparticles using the following relation (equation 8):

$$\alpha \approx \frac{1}{d}\ln\left(\frac{1}{T}\right) \quad (8)$$

where *d* is the thickness, *T* the transmittance and α the absorption edge. The theory of optical absorption gives the connection between the absorption coefficient α and the incident photon energy was given in equation (9):

$$\alpha h\nu = A\left(h\nu - E_g\right)^m \quad (9)$$

where *A* is energy dependent constant, $h\upsilon$ is photon energy, E_g is an energy band gap and *m* is an integer depends on the nature of electronic transitions. The prepared copper oxide nanoparticle is a wide band gap semiconductor material with a direct band gap.

Figure 4 (a) shows a strong fundamental absorption edge of the CuO nanoparticles lies in the UV spectral region with the wavelength approximately at 296 nm due to direct transition of electrons.

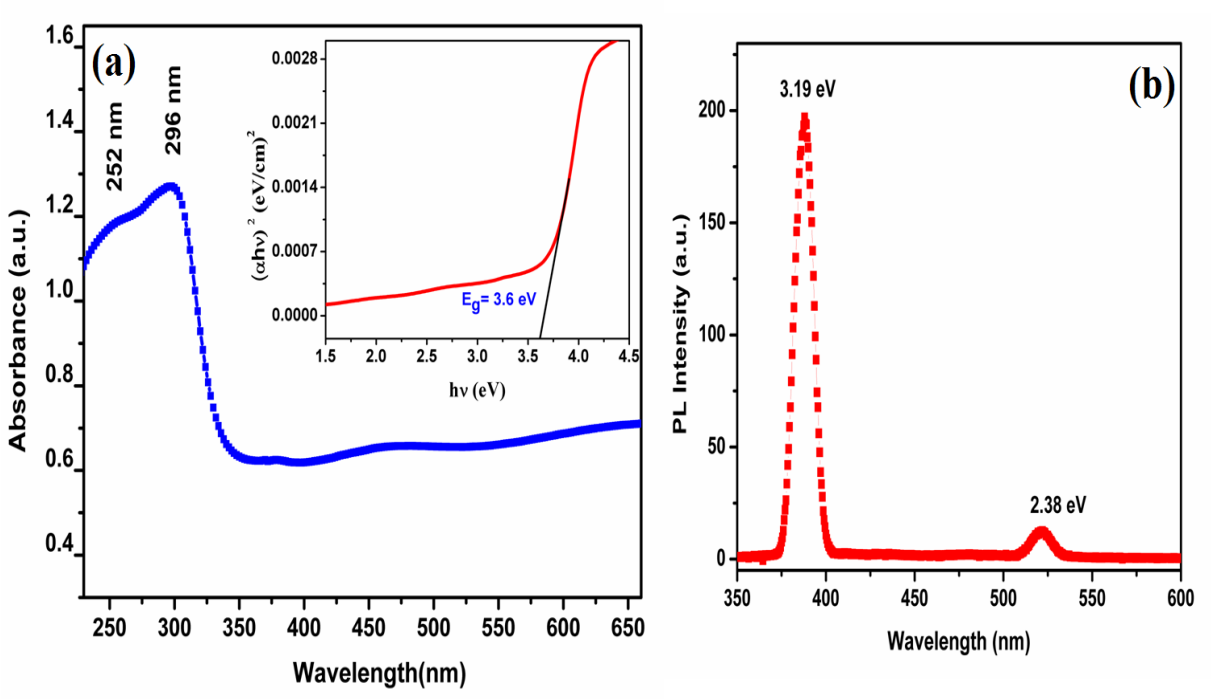

Figure 4. *(a) Absorption spectrum of synthesized CuO nanoparticles.* ***(insight)*** *Band gap of synthesized CuO nanoparticles. (b) Photoluminescence spectrum of synthesized C uO nanoparticles.*

Typically the UV absorption peak of CuO will lie between 280nm to 360nm. The UV absorption peak for CuO synthesized by a traditional chemical method was found to be 289 nm [21].

The calculated direct band gap value of the prepared nanoparticles is as shown in the insight plot of Figure 4 (a). is 3.6 eV, which was higher than the bulk band gap value (3.5 eV). At this point, simply direct transition-related absorption was observed, which shows that the direct band gap value is higher; hence the prepared material will be crystalline in nature which is in good agreement with the XRD pattern. The observed increasing band gap value of the prepared nanopaticles might be attributed to the presence of intragap states and quantum confinement effect [33].

Photoluminescence is an important analysis to identify the prepared nano-particles quality and band gap. It is also used to understand the electron-hole surface recombinations and identification of impurity levels in the materials. Figure 4 (b) illustrates the PL spectrum of CuO nanoparticles, which indicate a deep level emission peak appearing at 520 nm corresponds to the green emission region is from the CuO crystal structure [34]. These deep level emissions are usually related to defects in CuO nanoparticles. CuO is an intrinsically p type semiconductor material owing to the presence of Cu vacancies. The current theoretical estimations indicate that Cu vacancies are the most stable changes in the CuO electronic structure. If not, oxygen vacancies or O_{Cu} antisite defects are possible reason for this emission while its formation energy is approximately same as the formation energy of Cu vacancies. The peak observed in green emission is generally agreed to the singly ionized oxygen vacancies [35]. The other two peaks were originated in the region of 350–475 nm and 725–850 nm and it was attributed to Cu_2O phase [36]. So it is good agreement with the observation of the peaks at 388 nm corresponds to near ultraviolet region and 790 nm relates to near infrared region which ascribed to Cu nanoparticles.

3.3. Functional Group Analysis:

FTIR spectrum was recorded to identify the functional groups relating to CuO which can be depicted by the peaks. FTIR transmission spectrum in the range of 400 to 4000 cm^{-1} for prepared CuO nanoparticle was shown in Figure 5. Peaks at 3446, 3558, 3315, 2922, 2852, 2347, 1579, 1463, 1383, 1383, 1107, 990, 864, 674, 617, 515 and 465 cm^{-1} are observed and it was assigned to N – H Stretch, O – H Stretch, O – H Stretch, C – H Stretch, C – H Stretch, O=C=O Stretch, N – O Stretch, C – H Bend, C – H Bend, C – O Stretch, C = C Bend, C – H Bend, Cu – O Stretch [7] , Cu – O Stretch, C – Br Stretch and C – I Stretch.

The absorption band in the range of 600 to 680 cm^{-1} provided the clearest evidence for the presence of the crystalline CuO nanoparticles. It showed two distinct strong peak at 674 and 617 cm^{-1} which were related to the Cu-O stretching of cubic structure. Thus the result of FTIR spectrum is in good agreement with XRD analysis. The reduction and stabilization of copper oxide nanoparticles in leaf extract was due to the presence of primary aliphatic amines ($C{-}NH_2$) which was observed by the peak at 1107 cm^{-1}. Similar observations were made for seed extract in [37].

3.4. Surface Morphological and Compositional Analysis

The surface morphology of the as-formed CuO nanparticles were studied using SEM analysis and it was recorded with low and high magnification range as shown in Figure 6 (a,b). SEM image depicted that the particles were slightly agglomerated but showed smooth surface and irregular shapes. All the particles were interconnected randomly with one another to form large network systems with irregular shapes and pores. At higher magnification, the presence of pores was clearly visible corresponding to a high specific surface area of CuO nanoparticles.

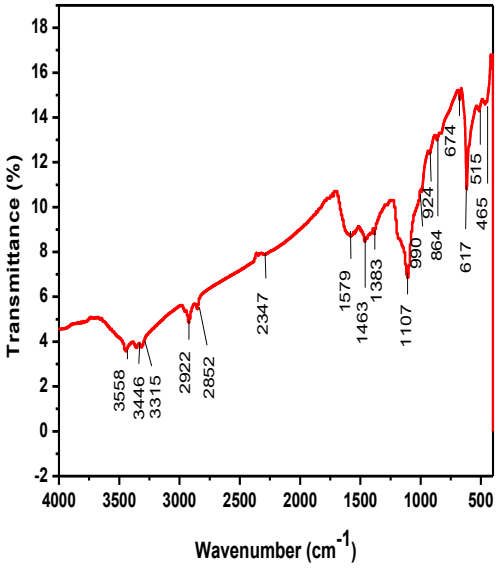

Figure 5. *FTIR transmission spectrum of synthesized CuO nanoparticles.*

SEM images confirmed that the final product consisted of a large number of CuO nanoparticle clusters. It showed the surface morphology as the combination of different shapes such as cube, square and spherical which was observed through low and high magnification resolution. The high magnified SEM image in Figure 6 (b). showed the presence of CuO nanoparticles which were individual cubic structure. The obtained cubic structure was in good agreement with XRD results.

The spherical morphological images are in agreement with the report available in literature using *Abutilon indicum* leaf extract [38], with some small differences, which may be due to the chemical composition.

The energy dispersive X-ray spectroscopy (EDX) studies revealed the chemical composition and formation of the synthesized CuO nanoparticles as shown in Figure 6 (c). EDX spectra confirmed the presence of constituents such as copper (Cu) and oxygen (O) in the nanoparticles. So it was clear from the EDX that the CuO nanoparticles were successfully -.

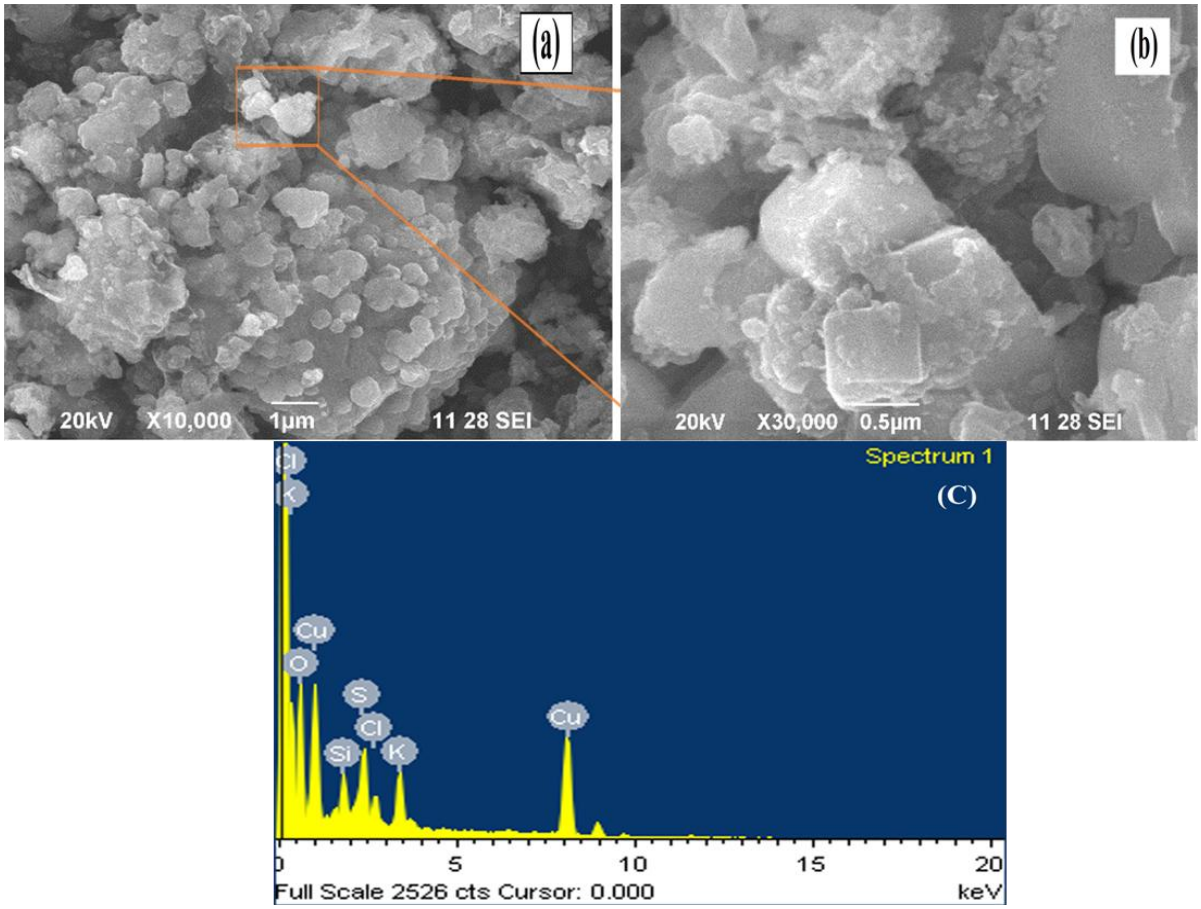

Figure 6. *(a,b) Low and high resolution SEM images of synthesized CuO nanoparticles, (c) Elemental composition of synthesized CuO nanoparticles.*

The peaks belonged to copper oxide which demonstrated that synthesized nanoparticles were crystalline in nature and the other impurity peaks such as Si, S, Cl and K were present which may be from the precipitates in the plant material [39].

3.5. Antimicrobial Activity Analysis

Antibacterial activity of the test sample was evaluated using the well diffusion method on Mueller-Hinton agar (MHA). The inhibition zones were reported in millimeters (mm). MHA agar plates were incubated with the test bacterial strain under aseptic conditions, wells (diameter= 6mm) were filled with different concentrations (10 µl, 20 µl, 30 µl and 40 µl) of the nanoparticle and incubated at 37°C for 24 hours. After the incubation period, the diameter of the growth inhibition zones was measured [40]. For the study, *Amikacin* (10 µg) was used as the standard antibiotic. *Fluconazole* (20 µg) was used as the standard antifungal agent. *Dimethyl sulfoxide* (DMSO) was utilized as negative control during preliminary experimental trials.

Nanoparticles possess high surface/ volume ratio, high dispersion and small crystallite size, which can easily interact with microbial surfaces. The large surface area of the nanoparticles improves their interaction with the microbes to carry out a wide range of antimicrobial activities [41]. *Staphylococcus aureus* was chosen to study the antibacterial activity of CuO nanoparticles as it is a human pathogen affecting our skin, respiratory and cardiovascular system causing several infections.

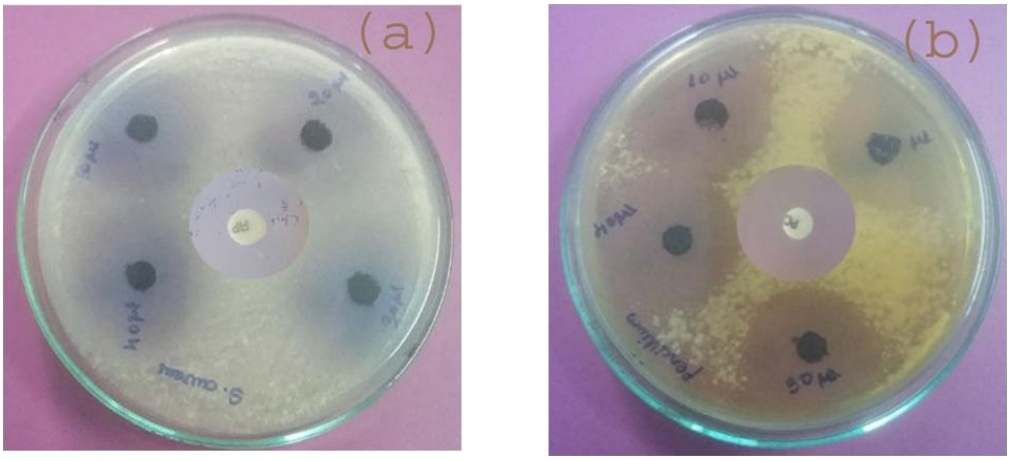

Figure 7. *Zones of inhibition of CuO nanoparticles against (a) Staphylococcus aureus and (b) Penicillium sp.*

The antibacterial activity of CuO nanoparticles against *Staphylococcus aureus* was evaluated for finding their role in antibacterial action as shown in Figure 7 (a). The prepared nanosized CuO nanoparticles were attached to the bacteria and distract the normal life of bacteria and therefore destruct rigorously to the outside surface of the bacteria such as proteins, lipids and DNA [38]. Table 3 showed that the inhibition zone of CuO nanoparticle was increased with increasing concentration and the maximum value of zone of inhibition was observed at 40 µl concentration. The occurrence of inhibition zone was an indication of absence of the growth bacteria on the plate. The interaction of bacteria and CuO ions released from nanoparticles caused adhesion and bioactivity due to electrostatic forces when it absorbed on the surface of the micro-organism's cell wall. This damaged the cell wall by killing the pathogens using their resistance property of synthesized nanoparticles against this micro-organism.

The efficiency of synthesized CuO nanoparticles was determined by the diameter of the clear zone in which the increasing diameter shows the increasing efficiency [42]. It proved that CuO nanoparticles are effective in killing a bacterial pathogen and it also showed higher antibacterial effect at higher concentration. The increase of bacterial resistance of CuO nanoparticles has been recognized as antimicrobials due to their excellent antimicrobial property.

Antifungal activities of sample were evaluated using the well diffusion method on Potato Dextrose agar. The inhibition zones were reported in millimeters (mm). The sample was dropped into the well at different concentrations 10 µl, 20 µl, 30 µl and 40 µl and incubated at 30°C for 48 hours. After the incubation period, the diameter of the growth inhibition zones was measured. *Penicillium* sp was chosen to study the antifungal activity of CuO nanoparticles. This fungus produces health complications like fever, asthma, etc. in the human body. The antifungal activity of the prepared CuO nanoparticle was shown in Table 3.

The prepared CuO nanoparticles resisted the growth of fungus due to the electrostatic attraction between fungus cell and nanoparticles. The release of Cu^{2+} ions of the nanoparticles can cause severe damage to the fungi by interacting with DNA and it also disturbed the electron transport which results in death of fungi. The size of the inhibition zone increased from 15 to 25 mm by increasing the concentration of the nanoparticles from 10 to 40 µl as shown in Figure 7 (b). This analysis confirmed that the diameter of the growth inhibition zone increased with the

concentration and the prepared CuO nanoparticles showed better activity at 40 µl. It was noted that an increase in CuO nanoparticle concentration also increased antifungal activity.

Table 3. *Antimicrobial activity of CuO nanoparticles synthesized from leaf extract.*

CuO concentration (µl)	Staphylococcus aureus bacteria	Penicillium sp. fungi
	Zone of inhibition (mm)	Zone of inhibition (mm)
10	20.3 ± 0.58	15.2 ± 0.29
20	25 ± 0.50	18.2 ± 0.29
30	28.3 ± 0.29	20 ± 0.50
40	30.3 ± 0.29	25.2 ± 0.58

The improved antifungal efficiency was observed in the high concentration of the CuO nanoparticles. The enhanced fungal inhibition may be due to the aspects such as morphology, size, specific surface area, etc. The effective activity of nanoparticle may be ascribed by its small crystallite size and large surface area which improves the adsorption of biomolecules and it destroy the fungi cell membrane more effectively. Thus it proved that the nanoparticles were strongly inhibited the growth of fungal pathogens suggesting the possibility of using as a fungicide. In comparison with earlier studies using chemically synthesized CuO nanoparticles, the biosynthesized CuO nanoparticles exhibits enhanced antibacterial activity against Gram-negative and Gram-positive bacterial strain, which is a significant feature for medical applications [20].

So this study proved that prepared copper oxide nanoparticles possess remarkable antimicrobial influence on *Staphylococcus aureus* and noticeable fungicidal influence on *Penicillium* sp. The antimicrobial effect of CuO nanoparticles tested against bacteria and fungus reveals that the prepared nanoparticles are very active as an antimicrobial agents. The results of antimicrobial activity suggested that CuO nanoparticles produced better activity by increasing the CuO concentration. Due to its antimicrobial activity; it can be incorporated in coatings, plastics, textiles, etc.

4. CONCLUSIONS

Copper oxide, CuO nanoparticles were prepared using green synthesis technique which reduces the addition of harmful chemical in this work. The crystallite size of CuO nanoparticles was calculated using Scherrer and Williamson-Hall method which showed good agreement with the value in the nanoscale range. The FTIR spectroscopic analysis revealed the presence of the functional groups responsible for the CuO Vibration. In UV-Visible spectroscopy, the green synthesized CuO nanoparticles showed an absorption peak around 296 nm and the calculated band gap value is 3.6 eV. Photoluminescence spectroscopy revealed that the observation of deep level emission peak at 520 nm corresponded to the green emission region which is from the CuO crystal structure. The high magnified SEM image showed the presence of cubic structure copper oxide nanoparticles, which is in good agreement with XRD results and the EDAX analysis confirm the presence of copper (Cu) and oxygen (O) in the prepared nanoparticles. The green synthesized CuO nanoparticles proved excellent antimicrobial activity against the pathogens paving its use in various fields like air and water filtration, antibacterial packing etc. Hence, it seems to be a promising application in biomedical field such as antimicrobial wound dressings and biomedicines.

ACKNOWLEDGEMENT

The authors wish to thank Sadakathullah Appa College, India for their financial support to carry out this research. We also thank Coimbatore Institute of Technology and Manonmaniam Sundaranar University

for providing XRD, UV, PL and SEM and other facilities.

CONFLICT OF INTEREST

The authors declare that they have no conflict of interest.

REFERENCES

1. Saranya, S., Vijayaranai, K., Pavithra, S., Raihana, N., Kumanan, K., "In vitro cytotoxicity of zinc oxide, iron oxide and copper nanopowders prepared by green synthesis", *Toxicol. Rep*, 4 (2017) 427–430.
2. Heydari, S., Shirmohammadi Aliakbarkhani, Z., Hosseinpour Zaryabi, M., "Photocatalytic Degradation of Safranin Dye from Aqueous Solution Using Nickel Nanoparticles Synthesized by Plant Leaves", *Int. J. Nanosci. Nanotechnol*., 16 (2020) 153-165.
3. Hadi, S.M., Bagherieh-Najjar, M.B., Kohan B.E., Mianabadi, M., "Ag-Conjugated Nanoparticle Biosynthesis Mediated by Rosemary Leaf Extracts Cor-rlates with Plant Antioxidant Activity and Protein Content", *Int. J. Nanosci. Nanotechnol*., 14 (2018) 319-325.
4. Ravichandiran, C., Sakthivelu, A., Davidprabu, R., Valanarasu, S., Kathalingam, A., Ganesh, V., Mohd. Shkir, Algarni, H., AlFaify, S., "In-depth study on structural, optical, photoluminescence and electrical properties of electrodeposited Cu_2O thin films for optoelectronics: An effect of solution pH", *Microelectron. Eng*, 210 (2019) 27–34.
5. Lu, Q., Wang, X., Yu, J., Feng, F., Yin, L., Kang, Y., Luo, H., "Synthesis of spindle-like CuO nanoparticles by using cathode glow discharge electrolysis plasma", *Mater. Lett*, 264 (2020) 127316.
6. Duraipandi Devi Priya, Selvaraj Mohana Roopan, Sehajpreet Singh, Jatin Bansal, Shajahan Shanavas, Maksudur Rahman Khan, Naif Abdullah Al-Dhabi, Mariadhas Valan Arasu, Veeramuthu Duraipandiyan, "Phyto-synthesis of CuO nano-particles and its catalytic application in C-S bond Formation", *Mater. Lett.*, 266 (2020) 127486.
7. Arunkumar, B., Johnson Jeyakumar, S., Jothibas, M., "A sol-gel approach to the synthesis of CuO nanoparticles using Lantana camara leaf extract and their photo catalytic activity", *Optik - International Journal for Light and Electron Optics*, 183 (2019) 698–705.
8. Davarpanah, S.J., Karimian, R., Goodarzi, V., Piri, F., "Synthesis of Copper (II) Oxide (CuO) Nanoparticles and Its Application as Gas Sensor", *Appl. Biotechnol. Rep*, 2 (2015) 329-332.
9. Paseban, N., Ghadam, P., Pourhosseini, P.S., "The Fluorescence Behavior and Stability of AgNPs Synthesized by *Juglans Regia* Green Husk Aqueous Extract", *Int. J. Nanosci. Nanotechnol*., 15 (2019) 117-126.
10. Mirzaei, S., Ghabooli, A., Mirzaei, M., "*Botrytis Cinerea*, One of the Most Destructive Plant Pathogens, as a Potent to Produce Silver Nanoparticles", *Int. J. Nanosci. Nanotechnol*, 16 (2020) 243-248.
11. Dudhane, A. A., Waghmode, S. R., Dama, L. B., Mhaindarkar, V. P., Sonawane A., Katariya, S., "Synthesis and Characterization of Gold Nanoparticles using Plant Extract of *Terminalia arjuna* with Antibacterial Activity", *Int. J. Nanosci. Nanotechnol*, 15 (2019) 75-82.
12. Pal, S., Mondal, S., Maity, J., Mukherjee, R. "Synthesis and characterization of ZnO nanoparticles using *Moringa oleifera* leaf extract: Investigation of photocatalytic and antibacterial activity", *Int. J. Nanosci. Nanotechnol*, 14 (2018) 111-119.
13. Ananda Murthy, H.C., Buzuayehu Abebe, Tegene Desalegn, Z., Prakash, C.H., Kumar Shantaveerayya, "A Review on Green Synthesis and Applications of Cu and CuO Nanoparticles", *Mat. Sci. Res. India*, 15(3), (2018) 279-295.
14. Phukan, S., Mahanta, A., Kakati, D., Rashid, M. H., "Green chemical synthesis of Pd nanoparticles for use as efficient catalyst in Suzuki-Miyaura cross-coupling reaction", *Appl. Organomet. Chem.*, 33 (2019) e4758.
15. Phukan, S., Kakati, D., Rashid, M. H., "Use of invasive weed to synthesize shape-tunable gold nanoparticles and evaluation of their catalytic activities in dye reduction", *Curr. Nanosci.*, 14 (2018) 511–519.
16. Gmach, J., Joachimiak, Ł., Błazewska, K. M., "aza-Michael addition of imidazole analogues", *Synthesis*, 48 (2016) 2681– 2704.
17. Chowdhury, R., Mollick, M. M. R., Biswas, Y., Chattopadhyay, D., Rashid, M. H., "Biogenic synthesis of shape-tunable Au-Pd alloy nanoparticles with enhanced catalytic activities", *J. Alloys Compd*, 763 (2018) 399–408.
18. Arunkumar, B., Johnson Jeyakumar, S., Jothibas, M., "A sol-gel approach to the synthesis of CuO nanoparticles using *Lantana camara* leaf extract and their photo catalytic activity", *Optik - International Journal for Light and Electron Optics*, 183 (2019) 698–705.
19. Raja Naika, H., Lingaraju, K., Manjunath, K., Danith Kumar., Nagaraju, G., Suresh, D., Nagabhushana, H., "Green synthesis of CuO nanoparticles using *Gloriosa superba* L.extract and their antibacterial activity", *Journal of Taibah University for Science*, 9 (2015) 7–12.
20. Muthuvel, A., Jothibas, M., Manoharan, C., "Synthesis of copper oxide nanoparticles by chemical and biogenic methods: photocatalytic degradation and in vitro antioxidant activity", *Nanotechnology for Environmental Engineering*, 5:14 (2020) 1-19.

21. Keabadile , O. P., Aremu, A. O., Elugoke, S. E., Fayemi, O. E., "Green and Traditional Synthesis of Copper Oxide Nanoparticles-Comparative Study", *Nanomaterials*, 10 (2020) 2502.
22. Zhang, D., Ni, X., Zheng, H., Li, Y., Wang, G., Yang, Z., "Synthesis of needle-like nickel nanoparticles in water-in-oil microemulsion", *Mater. Lett*, 59 (2005) 2011–2014.
23. Rakesh Chowdhury., Aslam Khan., Md. Harunar Rashid., "Green synthesis of CuO nanoparticles using *Lantana camara* flower extract and their potential catalytic activity towards the aza-Michael reaction", *RSC Advances*, 10 (2020) 14374.
24. Chieu D. Tran., James Makuvaza., Erik Munson., Brian Bennett., "Biocompatible Copper Oxide Nanoparticle Composites from Cellulose and Chitosan: Facile Synthesis, Unique Structure, and Antimicrobial Activity", *ACS Applied Materials & Interfaces*, 9:49 (2017) 42503-42515.
25. Biswajoy Bagchi., Sumit Dey., Suman Bhandary., Sukhen Das., Alakananda Bhattacharya., Ruma Basu., Papiya Nandy., "Antimicrobial efficacy and biocompatibility study of copper nanoparticle adsorbed mullite aggregates", *Materials Science and Engineering C*, 32 (2012) 1897–1905.
26. Mittal, D., Narang, K., Leekha Kapinder, A., Kumar, K., Verma, A. K., "Elucidation of Biological Activity of Silver Based Nanoparticles Using Plant Constituents of Syzygium cumini", *Int. J. Nanosci. Nanotechnol*, 15 (3), (2019) 189-198.
27. Brajesh Kumar., Kumari Smita., Luis Cumbal., Alexis Debut., Yolanda Angulo., "Biofabrication of copper oxide nanoparticles using Andean blackberry (Rubus glaucus Benth.) fruit and leaf", *Journal of Saudi Chemical Society*, 21 (2017) S475–S480.
28. Albert manoharan, A., Chandramohan, R., David prabu, R., Valanarasu, S., Ganesh, V., Shkir, M., Kathalingam, A., AlFaify, S., "Facile synthesis and characterization of undoped, Mn doped and Nd co-doped CuO nanoparticles for optoelectronic and magnetic applications", *J. Mol. Struct*, 1171 (2018) 388-395.
29. Hepzi Pramila Devamani, R., Alagar, M., "Synthesis and Characterisation of Copper II Hydroxide Nano Particles", *Nano Biomed. Eng*, 5 (3), (2013) 116-120.
30. Mote, V.D., Purushotham, Y., Dole, B.N., "Williamson-Hall analysis in estimation of lattice strain in nanometer-sized ZnO particles", *Journal of Theoretical and Applied* Physics, 6 (2012) 6.
31. Johnsy Arputhavalli, G., Agilan, S., Mahithosh Ray., Thangaraju, D., Marnadu, R., Chandrasekaran, J., Chandekar, K.V., Mohd. Shkir., Jebasingh, S., Dinesh, M., "Post-annealing effects on structural and magnetic properties of pulsed laser deposition grown Co–Ni–Al ferromagnetic shape memory alloys thin films", *Solid state sciences*, 111 (2021) 106493.
32. Dhineshbabu, N. R., Rajendran, V., Nithyavathy, N., Vetumperumal, R., "Study of structural and optical properties of cupric oxide Nanoparticles", *Appl Nanosci*, 6 (2016) 933–939.
33. Huang, C.Y., Chatterjee, A., Liu, S.B., Wu, S.Y., Cheng, C.L., "Photoluminescence properties of a single tapered CuO nanowire", *Appl. Surf. Sci*, 256 (2010) 3688–3692.
34. Anshuman Sahai., Navendu Goswami., Kaushik, S.D., Shilpa Tripathi., "Cu/Cu_2O/CuO nanoparticles: Novel synthesis by exploding wiretechnique and extensive characterization", *Appl. Surf. Sci*, 390 (2016) 974–983.
35. Ansar Mehmood., Ghulam Murtaz., Tariq Mahmood Bhatti., Rehana Kausar., "Phyto-mediated synthesis of silver nanoparticles from *Melia azedarach* L. leaf extract: Characterization and antibacterial activity", *Arab. J. Chem*, 10 (2017) S3048–S3053.
36. Reda Hassanien., Dalal Z. Husein., Mostafa F. Al-Hakkani., "Biosynthesis of copper nanoparticles using aqueous *Tilia* extract: antimicrobial and anticancer activities", *Heliyon*, 4 (2018) e01077.
37. Saranya Sukumar., Agneeswaran Rudrasenan., Deepa Padmanabhan Nambiar., "Green-Synthesized Rice-Shaped Copper Oxide Nanoparticles Using *Caesalpinia bonducella* Seed Extract and Their Applications", *ACS Omega*, 5 (2020) 1040−1051.
38. Faheem Ijaz., Sammia Shahid., Shakeel Ahmad Khan., Waqar Ahmad., Sabah Zaman., "Green synthesis of copper oxide nanoparticles using *Abutilon indicum* leaf extract: Antimicrobial, antioxidant and photocatalytic dye degradation activities", Tropical *Journal of Pharmaceutical Research*, 16 (4) (2017) 743-753.
39. Gomathi, M., Rajkumar, P.V., Prakasam, A., Ravichandran, K., "Green synthesis of silver nanoparticles using *Datura stramonium* leaf extract and assessment of their antibacterial activity", *Resource-Efficient Technologies*, 3 (2017) 280–284.
40. Shibana, A.T., Raiza, J., Pandian, K., "Amido-Amino Clay Stabilized Copper Nanoparticles: Antimicrobial Activity and Catalytic Efficacy for Aromatic Amination", *Int. J. Nanosci. Nanotechnol*, 16 (2020) 117-125.
41. Nallendran, R., Selvan, G., Balu, A.R., "NiO coupled CdO nanoparticles with enhanced magnetic and antifungal Properties", *Surfaces and Interfaces*, 15 (2019) 11–18.
42. Vala, A. K., Shah, S., "Rapid Synthesis of Silver Nanoparticles by a Marine-derived Fungus Aspergillus Niger and their Antimicrobial Potentials", *Int. J. Nanosci. Nanotechnol*, 8 (4), (2012) 197-206.